Modeling Urban Energy Supply Schemes

by

Bradley J. Tran

Bachelor of Science, Mechanical Science and Engineering
University of Illinois, Urbana-Champaign, 2011

Submitted to the Department of Architecture
in Partial Fulfillment of the Requirements for the Degree of

Master of Science in Building Technology
at the
Massachusetts Institute of Technology

June 2017

Signature of Author: Signature redacted
Department of Architecture
May 12, 2017

Certified by: Signature redacted
Christoph Reinhart
Associate Professor of Building Technology
Thesis Supervisor

Accepted by: Signature redacted
Sheila Kennedy
Professor of Architecture
Chair of the Department Committee on Graduate Students

Thesis Committee

Christoph Reinhart
Thesis Supervisor
Associate Professor of Building Technology
Department of Architecture
Massachusetts Institute of Technology

Leslie Norford
Professor of Building Technology
Department of Mechanical Engineering
Department of Building Technology
Massachusetts Institute of Technology

Modeling Urban Energy Supply Schemes

by
Bradley J. Tran

Submitted to the Department of Architecture
on May 12, 2017 in partial fulfillment of the requirements for the
Degree of Master of Science in Building Technology

Abstract

Rapid urbanization places increased pressure on governments and cities to use economical, low-carbon energy supply strategies. This manuscript details efforts to develop an integrated energy supply and demand analysis tool to help urban planners and designers evaluate and compare schemes to satisfy the electric, heating, and cooling demands of urban areas. Current simulation tools tend to focus on either the demand- or supply-side aspect of the energy challenges cities face. Additionally, these tools are often overly simplistic or complex with steep learning curves, rendering analyses directionally incorrect or inaccessible.

The developed framework integrates a 3D modeling platform, an industry-standard energy simulation engine, and variable-efficiency supply models to increase the accessibility and usability of results. This will help municipalities, developers, and urban planners make informed decisions related to energy supply schemes at the neighborhood level regarding estimated energy consumption, carbon emissions, and energy costs.

The approach is applied to case studies from six mixed-use neighborhood designs in three cities: Boston, Lisbon, and Kuwait City. The results illustrate the significance of using load- and temperature-dependent supply models instead of constant COP models. The results underscore the influence that weather, equipment, and regional power generation characteristics have on the optimal energy supply strategy for a given neighborhood design.

Thesis Supervisor: Christoph Reinhart
Title: Associate Professor of Building Technology

Acknowledgments

This thesis would not be possible without the generous contributions from many, and I am grateful for the encouragement I have received during my last 14 months at MIT. First, I would like to thank MIT and the Masdar Institute of Technology for providing the funding needed to complete this effort.

Professor Christoph Reinhart, my thesis supervisor, has provided thoughtful guidance and direction throughout the research and thesis-writing processes. I would also like to recognize Professor Leslie Norford for his intellectual support of this effort and willingness to serve as a reader. Michael Wetter and David Blum from Lawrence Berkeley National lab, as well as Professor Ahmed Ghoniem, Tea Zakula, and MIT's Gas Turbine Laboratory, lent their technical expertise on building and HVAC systems, helping me refine my research focus. Seth Kinderman and Pat Karalekas kindly provided data from MIT's combined cooling, heat, and power plant that I used to build a model to approximate a chiller's leaving condenser water temperature.

Extracting data from UMI was more challenging than I expected, and I appreciate the help that Alpha Arsano, Cody Rose, John Fechtel, and Renaud Danhaive provided. For the implementation of the energy supply models in Python, I owe a tremendous thanks to Michael Jermann, Will Setchell, and Jason Febery. Samuel Letellier-Duchesne, thank you for your efforts to integrate the Python code into UMI, as well as for the debugging help.

Accenture and the Connected Buildings team have been supportive of my decision to attend graduate school and flexible as I juggled my studies, research, and work. A special thank you to Sean Terry, Jay Hedley, Marty Newhouse, Megan Perrin, and Chuck Sloup for your support over these past two years. Balancing work and school has certainly been challenging, and I am confident that I would not be writing this had it not been for many of the individuals listed here. My personal trainer, Rob Watts, has helped me stay active despite my tendency to neglect my personal fitness when busy. Finding quick, healthy food is a challenge near MIT, and The Similans restaurant and staff deserve my gratitude for helping me eat well and feel like I have a home-cooked meal just a few minutes away.

I am thankful to have had the company and friendship of my lab mates and other campus friends. I am particularly grateful to have met Alpha, Renaud, and Toño Terán; you made my time at MIT so much more enjoyable, and I am honored to call you my friends. I look forward to returning to campus after graduation to return the favor while you complete your PhDs.

Finally, I would like to thank the Bros, Ashida family, and my family for your encouragement and love. Mike Jermann and Michael Ashida deserve special acknowledgement for taking countless late-night calls as I walked home from the lab. Thank you for your unwavering ability to cheer me up, regardless of my workload. To my partner, Jason, thank you for all your love and support since the beginning of the applications process. You were instrumental in my decision to apply, and you were always eager to hear about my work, regardless of how many times you have heard me talk about my research and machine learning course. I could not have completed this journey without you.

Grandma Reith and Grandpa Green, you stimulated and encouraged my interest in science and technology since I could crawl. I have learned a tremendous amount about fans, lighting, air conditioning systems, and so much more as a direct result of your generosity and enthusiasm for education. This passion you fueled continues to motivate me, and I am forever grateful. I dedicate this thesis to you.

Table of Contents

1 INTRODUCTION

Cities are responsible for approximately 75% of energy consumption and 80% of GHG emissions worldwide, and the continuing trend of urbanization will place increased pressure on cities to find creative approaches for curbing building-related emissions and energy consumption at competitive costs (UN, 2017). According to a recent report by the UN, the urban population is projected to grow by 2.5 billion from 2014 to 2050. Creutzig et al. estimate that this dramatic urbanization will result in a staggering threefold increase in energy consumption under a business-as-usual scenario. Encouragingly, the authors also found that urban planning and transport policies can limit this increase by 25% (Creutzig et al., 2014).

In addition to deliberate energy-efficient designs, energy use in the building sector can be reduced through two primary means: (1) by decreasing building energy demands through a combination of retrofits and commissioning and (2) by increasing the efficiency of the energy supply systems. Traditionally, individuals have concentrated on either developing planning tools focused on the building demand side or energy supply aspect, but few have integrated both dimensions (Keirstead et al., 2012). This bifurcation is largely the result of differences between key stakeholders. Building owners and tenants are responsible for purchasing energy from utilities and are therefore directly incentivized to minimize their consumption with little concern or control over the performance of the energy supply system.

Similarly, utilities focus on maximizing their profits, which may motivate them to improve the energy supply systems, but this often just involves the upkeep of existing infrastructure. Utilities do have influence over building energy demands, and they encourage energy efficiency improvements with rebates. However, these rebates neglect to improve the performance of the actual supply systems.

Municipalities, energy policy makers, and large campus administrators are well-positioned to encourage both reductions in building energy demands and improvements to the performance of energy supply systems to meet sustainability goals. Unfortunately, available simulation tools limit their ability to evaluate urban energy supply strategies within the context of building loads and impede the decision-making process. Current simulation tools either provide an overly simplistic analysis, or they are complex with steep learning curves that require detailed systems- and buildings- level modeling. A decision-making tool that provides fast, accurate results will help key stakeholders make more informed decisions.

In recent years, researchers have developed several bottom-up urban building energy models (UBEM) to address the need to provide an integrated method for evaluating building energy demands with energy supply strategies (Reinhart and Cerezo, 2016). Prominent examples include the City Energy Analyst from ETH Zurich, CitySim from Ecole Polytechnique Federale de Lausanne (EPFL), and the Urban Modeling Interface from the Massachusetts Institute of Technology.

The City Energy Analyst is an UBEM tool that allows users to analyze and optimize energy systems in neighborhoods and city districts. The tool integrates several database and computation modules with ArcGIS to allow users to compare urban design scenarios in conjunction with energy systems with respect to energy, carbon, and financial performance (Fonseca et al., 2015).

CitySim is a tool focused on simulating urban energy flows to help urban planners and stakeholders minimize the use of non-renewable energy sources (CitySim, 2017). This tool integrates several modules that approximate thermal and radiation loads, and couples them to plant and HVAC equipment models through a Java-based graphical user interface (GUI). These models include boilers, chillers, solar thermal systems, and energy conversion systems (Robinson et al., 2009).

The Urban Modeling Interface (UMI) is an urban environmental performance and analysis simulation platform (Reinhart et al., 2013). While the previously mentioned tools exclusively focus on operational energy use, UMI evaluates neighborhood performance across several dimensions from operational and embodied energy use to daylight access and neighborhood walkability. UMI's specific focus is to facilitate the design of holistic sustainability concepts for neighborhoods containing several hundred buildings.

UMI uses the Windows-based NURBS modeler Rhinoceros 3D as its geometric modeling platform. It links these geometric models of the buildings to a library containing building archetypes and an SQLite database to store results. UMI uses a clustering algorithm called the Shoeboxer (Dogan and Reinhart, 2017) that abstracts buildings of the same archetype into a series of perimeter and core models—or shoeboxes—for which hourly heating, lighting, cooling, and equipment simulations can be run using EnergyPlus's whole-building simulation engine (EnergyPlus, 2017).

The simplification of buildings into shoeboxes reduces the simulation time by up to two orders of magnitude in comparison to a full, multi-zone thermal simulation. Despite the dramatic reduction in simulation time, the results of using the Shoeboxer are comparable for homogenous buildings without atria and non-standard HVAC equipment. Since UMI was designed for use during master planning when little is known about the specifics of the buildings' interiors, the use of the Shoeboxer algorithm is justified for estimating the building load profiles.

Previous versions of UMI modeled building-level energy supply systems through simplified, constant-efficiency based equipment models. Given this approach neglects the effect that load and temperature have on equipment efficiency, the authors anticipated a need for a more sophisticated energy supply systems module that leverages hourly load data and allows for a more granular estimation of the performance of energy supply schemes. This presented an auspicious integration opportunity between UMI and the simulation framework presented in this manuscript.

This text details the modeling of four energy supply strategies and compares the use of constant efficiency models to dynamic ones whose efficiency is dependent on load and temperature. The authors applied these urban energy supply models to six neighborhood designs in three cities: Boston, Lisbon, and Kuwait City. The results illustrate the difference between the use of static and dynamic energy supply system models, as well as the importance weather, equipment, and regional power generation characteristics have on the choice of an optimal energy supply strategy with respect to energy consumption, carbon emissions, and costs.

2 METHODOLOGY

The authors developed models of four distinct energy supply systems and applied them to six neighborhood designs in three cities. The four strategies are described in Section 2.1. Sections 2.2, 2.3, and 2.4 review the HVAC models, losses, and key metrics used in simulating these four scenarios based on hourly cooling, heating, and non-HVAC electric loads. 2.5 introduces the six case studies and explains how the simulation results will be compared in the results portion of this text.

2.1 Energy Supply Strategies Introduction

The authors selected the following four energy supply schemes for their broad coverage of common types of urban energy supply systems in cities today. The key outputs from each model are the annual input energy required, associated carbon emissions, and the cost to purchase electricity and natural gas. Simplified diagrams illustrating the four scenarios are included below in Figure 1, Figure 2, Figure 3, and Figure 4.

Strategy 1: All-electric Grid

The United Nations Sustainable Energy for All Initiative—part of their 17 Sustainable Development Goals—seeks to double the current share of renewable energy sources by 2030 (UN, 2015). Additionally, the Energy Roadmap 2050 (EU, 2012) outlines six strategies for energy systems to reduce greenhouse gas emissions by 80% by 2050 (from 1990 levels). These strategies focus on the electrification of the heating sector (Connolly et al., 2014), and the authors expect an increase in the use of electric heat pumps to take advantage of the resulting low-carbon electricity.

For example, the UK's Committee on Climate Change has recommended a significant increase in the use of heat pumps as part of their strategy to meet the UK's 2050 greenhouse gas reduction targets (CCC, 2015). These policy goals provided the inspiration for modeling an all-electric energy supply scenario, which will likely gain wider adoption as other countries seek to decarbonize their electric grids and heating sectors.

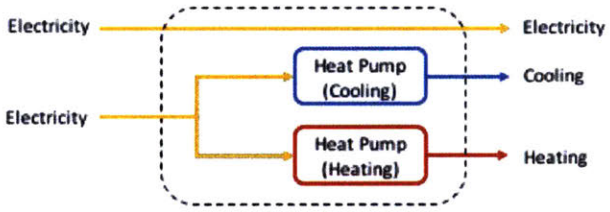

Figure 1: Simplified illustration of the all-electric grid scenario

Under this scenario, the electric grid supplies electricity to satisfy cooling, heating, and non-HVAC electric loads. The authors modeled this scenario such that the cooling and heating loads are satisfied using electric, air-source heat pumps located in each building. All electricity is purchased from the local grid, where the emissions factors, cost of generation, and 1st-law thermal efficiency of the power generation plants are dependent on the local utilities' energy supply mix.

The number of heat pumps for each building is based on the annual peak heating and cooling demands. For each hour, the fewest number of heat pumps required to meet the load are enabled, and all heat pumps evenly share the load. Because the size of the heat pumps is fixed, all enabled heat pumps will have the same PLR. For example, if the cooling load is 10 kW for a particular hour, and each heat pump has a maximum capacity of 3

kW, four heat pumps will be enabled, each providing an equal, 2.5kW contribution to satisfying the load.

Strategy 2: Electric + Natural Gas Grid

The next scenario represents a common method of providing space heating and cooling where the electric grid supplies electricity to satisfy cooling and non-HVAC electricity demands, and natural gas-fueled hydronic boilers provide heating for each individual building. Examples of this method of space heating and cooling can be found across the globe in cities like Chicago, New York, London, and Tokyo.

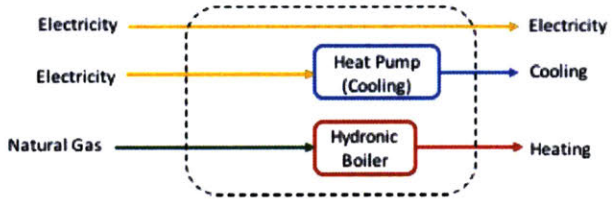

Figure 2: Illustration of the electric and natural gas grid scenario

The authors used the same heat pumps from the previous, all-electric grid strategy to provide cooling. Similar to the previous strategy, all electricity is purchased from the local grid and the number of heat pumps and boilers is based on annual peak cooling and heating demands. Again, the fewest number of equipment is enabled each hour, and the equipment evenly shares the load.

Strategy 3: Electric Grid + District Heating and Cooling Plant (DHC)

A recent United Nations Environment report noted that a 2013 survey of low-carbon cities worldwide revealed that district energy systems are a best-practice strategy for providing a low-carbon and affordable energy supply system (UNEP, 2016).

While district heating networks have been used in Europe as early as the 14th century (Rezai and Rosen, 2011), the first commercially viable district heating system appeared in Lockport, New York in 1877. Today, district heating accounts for ~13% of the EU's space heating needs (Connolly et al., 2014) and satisfies approximately 50% of the heating demands in a handful of countries, including Denmark, Finland, Sweden, Estonia, Latvia, Lithuania, Poland, Russia, and Iceland (Werner, 2017).

One of the first large district cooling networks was built to serve the Rockefeller Center in New York City, and by 1996, about 20 cities and towns used district cooling systems in the U.S. Europe's first district cooling systems did not appear until the 1960s in Paris, after which Finland, Germany, Italy, and Sweden adopted similar systems. Japan began using district cooling in the 1970s, and by 2005, there were over 154 networks within the country. More recently, the Middle East has begun using district cooling to serve densely populated areas with high cooling loads (Gang et al., 2016).

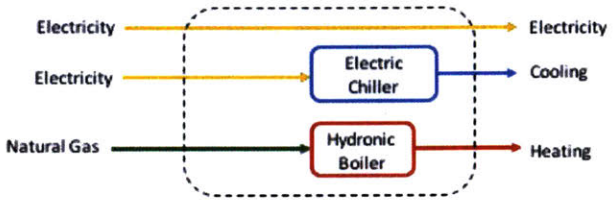

Figure 3: Simplified illustration of two major components in a district heating and cooling plant

Again, electricity from the grid satisfies non-HVAC electric demands, but now, a district cooling and heating (DHC) plant produces hot and chilled water to meet the cooling and heating loads. The DHC plant uses natural gas boilers to produce hot water and electricity from the grid to power centrifugal chillers and cooling towers to produce chilled water. Electric pumps distribute the hot and chilled water to the individual buildings.

The number of chillers and boilers is determined by the peak demands of the urban area, and the fewest number needed to meet the hourly heating and cooling demand is enabled.

Strategy 4: Combined Cooling, Heat, and Power

District Heating and Cooling is often paired with electricity generation, which is referred to as Combined Cooling, Heat, and Power (CCHP), or trigeneration. This centralized production of electricity, hot water/steam, and chilled water takes advantage of heat from the power generation process—or some other industrial process—that would be otherwise wasted (Chicco and Mancarella, 2008). These sorts of systems are often found on campuses in North America (IDEA, 2005) or at industrial sites that produce significant excess heat like paper mills or waste incinerators.

While the European Union is focused on promoting all-electric grids, the International Energy Agency (IEA) notes that CCHP technologies can play a fundamental role in a low-carbon economy (IEA, 2014).

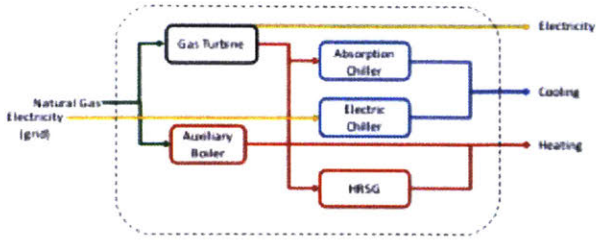

Figure 4: Major components of the modeled CCHP plant

The CCHP plant operates to satisfy all cooling, heating, and electric loads for the urban area, and the simplified model consists of a gas turbine, electric generator (not pictured), and the HVAC equipment needed to produce and distribute hot and chilled water. Waste heat from the gas turbine is diverted to an absorption chiller and heat recovery steam generator (HRSG) to provide heating and cooling. Natural gas boilers and electric centrifugal chillers provide supplemental heating and cooling when the waste heat is insufficient to meet the heating and cooling loads of the urban area.

The gas turbine and generator are sized to meet peak electrical demand, and they follow the electrical load. Waste heat from the turbine first satisfies the urban area heating load, and then cooling demands.

The number of absorption chillers equals the minimum number of chillers needed to utilize the peak amount of recoverable heat minus the amount of heat used for satisfying heating loads. Similarly, the number of electric centrifugal chillers equals the minimum number of chillers needed to satisfy the peak supplementary cooling demand. As in the last three scenarios, the fewest number of devices are enabled to meet the hourly loads, and all equipment evenly shares the load.

2.2 Equipment Models Overview

Each of the four energy supply strategies rely on the use of models to approximate the efficiency of the equipment needed to meet the cooling, heating, and electrical demands. This approximation influences the estimated annual input energy, emissions, and cost associated to each scenario. Table 1 includes the energy supply strategies and the corresponding equipment models used.

Table 1: Equipment Models Used for Each Supply Strategy

Equipment Model	Electric Grid	Grid + NG	Grid + DHC	CCHP Plant
Heat Pump (Cooling Mode)	X	X	-	-
Heat Pump (Heating Mode)	X	-	-	-
Natural Gas Boiler	-	X	X	X
Electric Centrifugal Chiller	-	-	X	X
Absorption Chiller	-	-	-	X
Cooling Tower	-	-	X	X
Gas Turbine	-	-	-	X

2.2.1 Constant-efficiency Equipment Models

The authors first implemented the constant-efficiency variants the four energy supply strategies. The use of these types of models simplifies the calculations needed to estimate annual energy consumption, emissions, and operational costs. See Table 2 for a listing of the constant efficiency values and coefficients of performance (COP) used.

Table 2: Constant Efficiency Values Used

Equipment Model	Efficiency
Heat Pump (Cooling Mode)	3.81 COP
Heat Pump (Heating Mode)	3.90 COP
Natural Gas Boiler	80%
Electric Centrifugal Chiller	8.11 COP
Absorption Chiller	1.39 COP
Natural Gas Turbine	40%

The selected constant efficiency values are based on the corresponding temperature- and load-dependent models' nominal efficiency as presented in section 2.2.2.

2.2.2 Variable-efficiency Equipment Models

The authors also implemented dynamic, load- and/or temperature-dependent equipment models. This section details the selected models previously outlined in Table 1.

Heat Pump (Cooling Mode)

The researchers selected a first-principles model based on the work of (Zakula, 2013) to approximate the COP

of a heat pump in cooling mode. Zakula performed a static optimization[1] of a steady-state model with cooling load, zone drybulb temperature, and outside air drybulb temperature as optimization input parameters.

The following equation approximates COP as a function of part load ratio and outside air drybulb temperature:

Equation 1: Heat Pump (Cooling Mode) COP

$$COP = (3.02\,E^{-3} - 3.23\,E^{-1}plr + 1.23\,E^{-2}db + 4.76\,E^{-1}plr^2 - 2.38\,E^{-4}plr * db - 2.86\,E^{-4}db^2 - 2.02\,E^{-1}plr^3 + 6.77\,E^{-4}plr^2 * db + 3.71\,E^{-5}plr * (db^2 + 4.25\,E^{-6}db^3)^{-1}$$

Where

plr is the part load ratio

db is the outside air drybulb temperature in Celsius

Refer to Appendix 6.1, Table 9 for the specifications of the heat pump.

Heat Pump (Heating Mode)

The authors selected a regression-based model to approximate the performance of a variable-speed, ductless heat pump in heating mode. The Purdue researchers who published this model found that the heating capacity and heat pump power input were both linear functions of the outdoor drybulb temperature (Cheung and Braun, 2010).

Although this model was developed across a range of outdoor air drybulb temperatures, the final, published model is solely dependent on part load ratio. The authors used this model to estimate the heat pump's COP under varying load conditions.

Equation 2: Heat Pump (Heating Mode) Work

$$W = W_{max}\left[C_0 + C_1 * plr + C_2 * plr^2 + C_3 * plr\left(\frac{V}{V_{max}}\right) + C_4 * plr^3 + C_5\left(\frac{V}{V_{max}}\right)^3 + C_6 * \left(\frac{V}{V_{max}}\right)\right]$$

Where

W is the heat pump's energy input

W_{max} is the max energy input to the heat pump

plr is the part load ratio

$\frac{V}{V_{max}}$ is the ratio of the evaporator fan's speed to max speed and is assumed to be 1

The authors calculated the COP of the heat pump using Equation 3, below.

Equation 3: COP Calculation for Heat Pump, Heating Mode

$$COP = \frac{HeatingLoad}{W}$$

Table 9 and Table 10 of the appendix list the coefficients the authors used in Equation 2, and it includes specifications for the heat pump.

Natural Gas Boiler

The authors selected the new style, low-temperature boiler from EnergyPlus. This model approximates boiler efficiency using a cubic equation with part load ratio as an input. The nominal efficiency is 80%, regardless of boiler size, and the minimum part load ratio is 10%. Additionally, the model does not specify a low-temperature limit on the boiler.

The authors used the following equation to approximate the efficiency of the boiler:

Equation 4: Boiler Efficiency

$$n_{boiler} = n_{boiler,nom} * X_b$$

Where

n_{boiler} is the calculated efficiency of the boiler

$n_{boiler,nom}$ is the nominal efficiency of the boiler (80%)

X_b is the boiler efficiency modifier given by the following equation:

Equation 5: Boiler Efficiency Modifier

$$X_b = c1 + c2 * plr_b + c3 * plr_b^2 + c4 * plr_b^3$$

Where

plr_b is the part load ratio of the boiler

[1] Matching of compressor, fan, and pump speeds to needed heat pump capacity (ASHRAE, 2011, Chapter 42).

Refer to Appendix 6.1, Table 12 for the coefficients used in Equation 5.

Electric Centrifugal Chiller

The authors selected the ReformulatedEIR EnergyPlus electric chiller model to approximate chiller efficiency under varying load and temperature conditions. This model was developed by (Hydeman et al., 2002), and it is based on chiller performance data at reference conditions in conjunction with three curve fits. The three performance curves are as follows:

1. CapFunT: Cooling capacity as a function of temperature
2. EIRFunT: Energy input to cooling output ratio as a function of temperature
3. EIRFunPLR: Energy input to cooling output ratio as a function of part load ratio (EnergyPlus Engineering Reference, 14.3.10.2)

Equation 6: CapFunT, Centrifugal Chiller

$$CapFunT = a + b(T_{evap,l}) + c(T_{evap,l})^2 + d(T_{cond,l}) + e(T_{cond,l})^2 + f(T_{evap,l})(T_{cond,l})$$

Equation 7: EIRFunT, Centrifugal Chiller

$$EIRFunT = a + b(T_{evap,l}) + c(T_{evap,l})^2 + d(T_{cond,l}) + e(T_{cond,l})^2 + f(T_{evap,l})(T_{cond,l})$$

Equation 8: EIRFunPLR, Centrifugal Chiller

$$EIRFunPLR = a + b(T_{cond,l}) + c(T_{cond,l})^2 + d(plr_{CC}) + e(plr_{CC})^2 + f(T_{cond,l})(plr_{CC}) + g(T_{cond,l})^3 + h * (plr_{CC})^3 + i * (T_{cond,l})^2(plr_{CC}) + j * (T_{cond,l})(plr_{CC})^2$$

Where

$T_{evap,l}$ is the temperature of the water leaving the chiller's evaporator and sent to the buildings

$T_{cond,l}$ is the temperature of the water leaving the chiller's condenser and returned to the cooling towers

plr_{CC} is the part load ratio of the centrifugal chillers

Performance curves can be produced for specific chillers by fitting either a chiller's manufacturer's data or by using measured data from the chiller. EnergyPlus includes a library of over 100 centrifugal, screw, and scroll chiller models and their associated coefficients for the three performance curves. The authors selected a McQuay PEH series chiller for use in the case studies presented in this paper. This centrifugal chiller has a high COP, broad leaving condenser water temperature range, and modest size, which are characteristics the authors anticipated would contribute to good performance of this chiller under a variety of scenarios.

Refer to Appendix 6.1, Table 13 for the coefficients used in Equation 6, Equation 7, and Equation 8. See Table 14 for the centrifugal chiller specifications.

This centrifugal chiller model uses the leaving evaporator and leaving condenser water temperatures as inputs. The leaving evaporator temperature is assumed to be constant at 4.44 °C (40 °F), and the leaving condenser water temperature is based on the outside air drybulb temperature and chiller PLR.

The researchers used Equation 9 to approximate the leaving condenser water temperature, commonly referred to as the condenser water return temperature. Explicitly, this is the temperature of the water leaving the chiller's condenser and returned to the cooling towers.

Equation 9: Condenser Leaving Water Temperature

$$T_{cond,l} = C1 + C2 * db^2 + C3 * db * PLR_{CC}$$

Where

db is the outside air drybulb temperature in Celsius

PLR_{CC} is the part load ratio of the centrifugal chillers

Equation 9 was found by creating a linear regression model using temperature and load data from the central plant chillers at the Massachusetts Institute of Technology in Cambridge, Massachusetts. The researchers selected a second-order polynomial fit with an R^2 error of 0.55.

Refer to Appendix 6.1, Table 15 for the coefficients used in Equation 9.

The authors used the following equations to estimate the hourly energy consumption of the chiller (Hydeman et al., 2002).

Equation 10: Centrifugal Chiller Modifier

$$X_{cc} = CapFunT * EIRFunT * EIRFunPLR$$

Equation 11: Centrifugal Chiller Energy

$$Energy_{cc} = X_{cc} * Power_{cc,nom}$$

Where

X_{cc} is the centrifugal chiller modifier that results from multiplying the three performance curves together

$Energy_{cc}$ is the energy consumed by the centrifugal chiller

$Power_{cc,nom}$ is the rated, nominal power of the chiller specified in Table 14

Absorption Chiller

The absorption model selected is included in EnergyPlus' library of DataSets within the file labeled ExhaustFiredChiller.idf. It is a direct-fired, two-stage absorption chiller which is based on the ABSORG-CHLR model from DOE-2.1 (EnergyPlus Engineering Reference, 14.3.10.2)

Similar to the centrifugal chiller, the absorption chiller model uses performance information at design conditions in conjunction with three performance curves. The three performance curves are as follows:

1. AbsCapFunT: Cooling capacity as a function of temperature
2. TeFIRFunT: Thermal energy input to cooling output ratio as a function of temperature
3. TeFIRFunPLR: Thermal energy input to cooling output ratio as a function of part load ratio

Equation 12: CapFunT, Absorption Chiller

$$AbsCapFunT = a + b(T_{evap,l}) + c(T_{evap,l})^2 + d(T_{cond,e}) + e(T_{cond,e})^2 + f(T_{evap,l})(T_{cond,e})$$

Equation 13: TeFIRFunT, Absorption Chiller

$$TeFIRFunT = a + b(T_{evap,l}) + c(T_{evap,l})^2 + d(T_{cond,e}) + e(T_{cond,e})^2 + f(T_{evap,l})(T_{cond,e})$$

Equation 14: TeFIRFunPLR, Absorption Chiller

$$TeFIRFunPLR = a + b(PLR_{ac}) + c(PLR_{CC})^2$$

Where

$T_{evap,l}$ is the temperature of the water leaving the chiller's evaporator

$T_{cond,e}$ is the temperature of the water entering the chiller's condenser and is estimated based on a constant offset from the previously calculated $T_{cond,l}$. Specifically,

Equation 15: Entering Condenser Water Temperature

$$T_{cond,e} = T_{cond,l} - \Delta_{cond}$$

Δ_{cond} is the difference between the entering and leaving condenser water temperature—assumed to be a constant 11 °C.

PLR_{ac} is the part load ratio of the absorption chiller

Refer to Appendix 6.1, Table 16 and Table 17 for the coefficients used in Equation 12, Equation 13, and Equation 14, as well as for the absorption chiller specifications.

The following set of equations compute the energy consumed by the absorption chiller.

Equation 16: Absorption Chiller Modifier

$$X_{ac} = AbsCapFunT * TeFIRFunT * TeFIRFunPLR$$

Equation 17: Absorption Chiller Energy

$$Energy_{ac} = X_{ac} * Capacity_{ac,nom}$$

Where

X_{ac} is the absorption chiller modifier

$Energy_{ac}$ is the energy consumed by the absorption chiller

$Capacity_{ac,nom}$ is the nominal, rated capacity of the absorption chiller

Cooling Tower

The authors selected a cooling tower model used by (Fonseca et al., 2016) in their City Energy Analyst Paper. The model is based on the work done by (Bertagnolio, 2012) who modified an epsilon-NTU method from (Lebrun et al., 2002). This epsilon-NTU method was combined with cooling tower data collected from a market survey to estimate the fan and pump energy associated to the cooling towers.

The following equation relates the estimated cooling tower energy consumption to chiller part load and the nominal power consumption of the cooling tower.

Equation 18: Cooling Tower Energy

$$CT_{EE} = (0.8603 * PLR_{CC}^{3} + 0.2045 * PLR_{CC}^{2} - 0.0623 * PLR_{CC} + 0.00626) * CT_{EE,Nom}$$

Where

$CT_{EE,Nom}$ is the nominal energy concumption of the cooling towers, or specifically,

Equation 19: Cooling Tower Nominal Energy Consumption

$$CT_{EE,Nom} = 0.011 * CC_{Capacity,Nom}$$

Where

$CC_{Capacity,Nom}$ is the nominal capacity of the centrifugal chillers

Natural Gas Turbine

The authors selected a gas turbine model presented in a 2011 entry in the Journal of Engineering for Gas Turbines and Power. This model is the result of performing a curve fit on three sets of operational data from an actual gas turbine (Meybodi and Behnia, 2011). Equation 20 was presented by Meybodi and Behnia and relates the part load efficiency of the gas turbine to part load ratio and nominal efficiency.

Equation 20: Ratio of Gas Turbine Part-load and Rated, Nominal Efficiencies

$$\frac{\eta_{th,PL}}{\eta_{th,Nom}} = -6.343E^{5} * plr^{2} + 0.0137 * plr + 0.2626$$

Where

$\eta_{th,PL}$ is the part load efficiency of the gas turbine

$\eta_{th,Nom}$ is the rated, nominal efficiency of the gas turbine

plr is the part load ratio of the gas turbine

While Meybodi and Behnia did not specify a minimum part load ratio, the authors assumed a 40% PLR for the gas turbine model. This minimum PLR is between the rated minimum value for common gas turbines (GE, 2016). In addition, the gas turbine was assumed to be of the single-shaft variety with stoichiometric combustion under full-load conditions. Heat recovery was assumed to be 80% of the waste heat (Pilavachi, 2000) and no losses were assumed for the electric generator because of the high efficiency ~99% of modern electric generators (Siemens, 2017).

2.3 Distribution Losses + Auxiliary Equipment Energy

The authors approximated transmission losses and energy consumption from auxiliary equipment for each of the four energy supply schemes. Table 3 below summarizes which category of losses and auxiliary energy were included by scenario.

Table 3: Losses and Auxiliary Equipment Energy Associated to the Energy Supply Strategies

Model	Electric Grid	Grid + NG	Grid + DHC	CCHP Plant
Electrical Transmission Losses	X	X	X	X
Heat Losses	-	-	X	X
Pumping Energy	-	-	X	X
Cooling Towers	-	-	X	X

2.3.1 Electrical Transmission and Distribution Losses

Energy is lost due to heat dissipation during transmission from the generating station to the urban areas where the electricity is consumed. The average transmission and distribution losses for each of the three locations was found and is summarized in Table 4.

While the authors applied transmission and distribution losses to electricity purchased from the grid in the CCHP scenario, they assumed electricity produced by the CCHP plant to have negligible losses due to its close proximity to the modeled urban area.

2.3.2 Heat Losses

As hot or chilled water is distributed via pipes to the buildings of an urban area, heat exchange with the environment results in losses. The authors assumed losses of 10% of the total heat delivered from hot or chilled water for the DHC and CCHP scenarios (Mancarella, 2012). They did not consider heat losses for the all-electric grid and electric grid and natural gas scenarios where the HVAC equipment is located in each building.

2.3.3 Pumping Energy

The authors estimated constant pumping energy requirements as 0.5% of the heat delivered for heating and 2.0% of the heat removed for cooling for the DHC and CCHP scenarios (Frederiksen and Werner, 2013).

2.4 Description of Key Metrics

Annual input energy, carbon emissions, and energy costs are the primary metrics the authors selected to compare the four energy supply strategies. This portion of the text details the approach the authors used to calculate these metrics, as well as a few others that are used in the results section.

Annual Input Energy

This represents the total amount of source energy required to satisfy the non-HVAC, heating, and cooling loads of the urban area. This metric accounts for all equipment energy, losses, and the efficiency of electricity generation.

Annual Carbon Emissions

This value represents the amount of carbon emissions produced in satisfying an urban area's loads. It includes the emissions tied to electricity production and the combustion of natural gas in boilers and gas turbines.

Annual Energy Cost

This figure represents the total cost of electricity and natural gas needed to meet an urban area's demands. The authors used the prices listed in Table 4 in conjunction with the input energy needed to calculate this metric.

Heating and Cooling System Efficiency

These metrics denote the overall efficiency of the heating and cooling systems employed. More specifically, the authors calculated these values by dividing the heating or cooling load by the input or source energy needed to satisfy that demand.

Coefficient of Performance (COP)

The authors calculated the annual efficiency of each of the pieces of equipment used in the energy supply strategies and compared them to the nominal, rated efficiency. COP is simply the annual sum of the heat moved or generated divided by the total input energy to the device.

2.5 Case Studies

The authors applied both the constant- and variable-efficiency sets of four energy supply scenarios to six neighborhood designs in Boston, Lisbon, and Kuwait City. Students in a graduate-level course at MIT designed and modeled these neighborhoods with Rhino and UMI, with the intent to develop a sustainable design for a mixed-use neighborhood. See Figure 5 for an example neighborhood design from one of the neighborhoods located in Kuwait City.

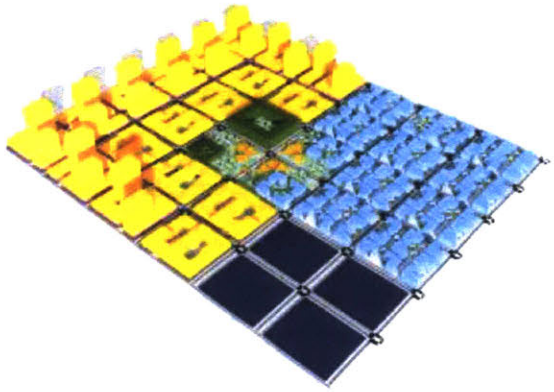

Figure 5: Mixed-use neighborhood in Kuwait City with commercial, office, and residential spaces. Yellow represents mixed use buildings, and the light blue structures are single-family residences.

The authors needed several key input parameters for each of the cities to apply their proposed framework. See Table 4 for a summary of these inputs.

Table 4: Region-specific parameters[2]

Input Parameters	Boston	Lisbon	Kuwait City
Price of Electricity (USD/kWh)	$0.17	$0.25	$0.01
Price of Natural Gas (USD/kWh)	$0.038	$0.1	$0.0098
Electrical Generation Efficiency (%)	33.4%	48.2%	26.9%
Electrical Transmission Losses (%)	5.0%	10.6%	11.7%
Emissions Factor (Metric Tons CO2/kWh generated)	4.45E-4	2.81E-4	7.27E-4

After applying the framework to the six case studies, the authors recorded the key model outputs which are referenced in Section 2.4.

Electrical Grid Generation Efficiency

The authors estimated efficiency factors for the electrical generation mix for Boston, Lisbon, and Kuwait City based on published data from the U.S. Energy Information Administration on the typical

[2] See Table 20 in the appendix for sources.

efficiencies of electrical generation methods in conjunction with the mix of electrical generation types for Massachusetts, Portugal, and Kuwait.

The authors used 2015 data from U.S.-based power plants to estimate the efficiency for both fossil-fueled and nuclear generating stations (EIA, 2015), as well as for renewables (EIA, 2011).

Table 18 and Table 19 of Appendix 6.2 include a summary of the reported values for the efficiency of various electrical generation sources and the power generation mix for Boston, Lisbon, and Kuwait City. For Boston, the authors assumed the same generation mix as for Massachusetts, and for Lisbon and Kuwait City, the authors used the average power generation mix for their respective countries.

2.6 UMI and Rhino Integration

The authors collaborated with a colleague to integrate their Python code into UMI to allow greater accessibility of the tool and its results. With this integration, users can quickly compare supply strategies for different urban areas by modeling a neighborhood in Rhino, running UMI's energy simulation, and choosing to run the energy supply tool. The tool displays results in the Rhino command line, and it automatically saves several .CSV files with detailed results to the users' neighborhood's working directory.

3 RESULTS

3.1 Constant vs. Variable-efficiency Results

The authors applied both the constant- and variable-efficiency models to the six neighborhood designs to (1) compare the difference in predicted energy consumption, carbon emissions, and energy cost, and, more interestingly, to (2) determine whether the selected model type materially changes the results.

Of the 72 comparisons (6 neighborhoods x 4 energy supply strategies x 3 metrics) between the constant- and variable-efficiency models, the constant-efficiency models under predicted the results approximately 89% of the time relative to the variable models. In only 8 of the comparisons did the constant-efficiency models over predict, and this was by a small margin of ~1% or less.

Table 5 shows the calculated percent difference between the average COP for the variable efficiency equipment models and the nominal values. Except for the heat pump in cooling mode, using the constant-efficiency models under-predicts the efficiency of the equipment models—and, therefore, the energy consumption, emissions, and cost as well.

Not surprisingly, the difference in average COPs for the pairs of neighborhoods in the same city was minimal. Even looking between cities, the difference in the calculated COPs do not vary dramatically by equipment model, particularly for the boilers, absorption chiller, and gas turbine.

Table 5: List of average COPs for each equipment model by case study and a percent difference between the average variable COPs and the nominal ones

Model	B1	B2	L1	L2	K1	K2	Avg	Nom	% Diff
HP, Cool	7.4	7.6	6.5	7.0	6.3	6.1	6.8	3.8	79%
HP, Heat	2.3	2.4	3.2	2.3	2.4	3.0	2.6	3.9	-33%
Gas Boiler	0.7	0.7	0.7	0.7	0.7	0.7	0.7	0.8	-14%
Cen Chiller	7.2	5.6	7.1	7.3	7.6	7.7	7.1	8.1	-13%
Abs Chiller	1.0	1.0	1.0	1.0	1.0	1.0	1.0	1.4	-31%
Gas Turbine	0.3	0.3	0.3	0.3	0.3	0.3	0.3	0.4	-19%

B = Boston, L = Lisbon, and K = Kuwait City

Figure 6 shows the average difference for Boston and Lisbon is around 11% and 12%, whereas for Kuwait City, the difference is about 5% lower for energy and emissions.

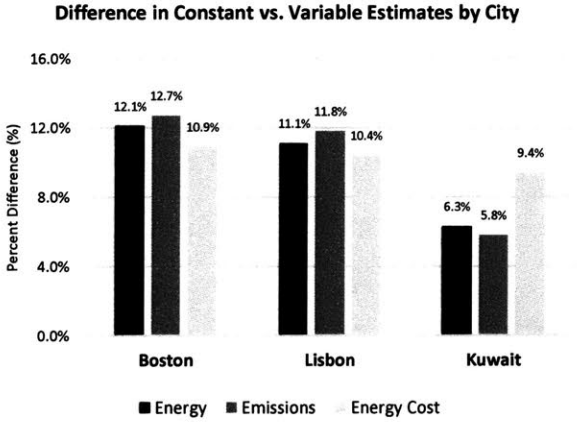

Figure 6: Graph illustrating the difference in predicted energy consumption, emissions, and energy cost by city.

A comparison by energy supply strategy highlights a dramatic difference in the predicted metrics for the CCHP plant of 21.7% and a minimal difference between the Grid + NG strategy of just 1.9%. The larger difference for the CCHP plant is likely because this strategy relies on the greatest number of models, which introduces additional opportunities for the results to diverge.

The difference between the predicted results for the All-electric Grid and District Heating and Cooling strategies were on average 11.5% and 5.1%, respectively. Note that the difference for energy, emissions, and cost are

identical for the all-electric scenario—and not the other three—because the differences are solely attributable to the parameters associated to the electric grid. See Figure 7.

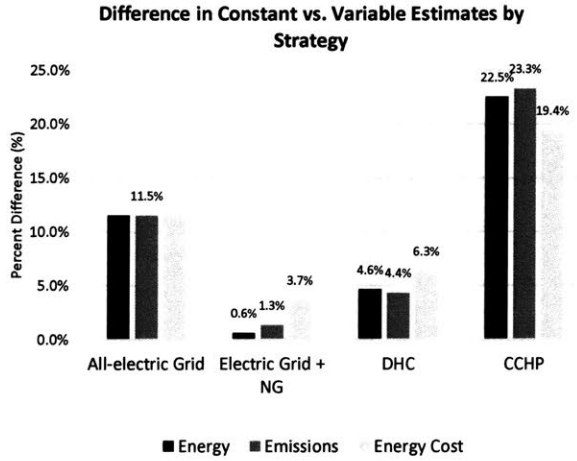

Figure 7: Graph of the percentage difference between the constant- and variable-efficiency model predictions by key metric and energy supply strategy.

More interesting than whether the predicted results vary is understanding whether the use of one type of model produces directionally different results than another. It does.

With respect to energy, the constant and dynamic models predict different best choices for both Boston neighborhoods. There is directional agreement between the optimal choices with respect to energy for the Lisbon neighborhoods, but the remaining rankings differ. For the Kuwait neighborhoods, the predicted energy consumption rankings are the same for the first and second choices, but reversed for the third- and fourth-place energy supply strategies.

The comparison for emissions yields similar results. The two methods predict the same optimal energy supply strategy for the Boston neighborhoods and different results for the second and third and fourth choices for Lisbon and Kuwait City, respectively.

Energy cost differences do not follow the same trends as energy and emissions. The constant and variable models predict different choices for the Boston and Lisbon neighborhoods, but agree on the top choice for the neighborhoods in Kuwait City.

See Table 6 for a summary comparing the predicted rankings for each of the energy supply strategies for both constant and variable models with respect to energy, carbon, and cost.

Table 6: Comparison of constant- and variable-efficiency models' predicted ranking of energy supply strategy by city and metric (1 is the optimal strategy)

Input Energy	B1		B2		L1		L2		K1		K2	
	C	V	C	V	C	V	C	V	C	V	C	V
All-electric Grid	2	4	1	4	1	1	1	1	3	4	3	4
Electric + NG Grid	4	1	3	2	4	2	4	2	4	3	4	3
DHC	3	3	4	3	2	3	3	3	2	2	2	2
CCHP	1	2	2	1	3	4	2	4	1	1	1	1

Emissions	B1		B2		L1		L2		K1		K2	
	C	V	C	V	C	V	C	V	C	V	C	V
All-electric Grid	2	2	1	2	1	1	1	1	3	4	3	4
Electric + NG Grid	4	1	3	1	3	2	3	2	4	3	4	3
DHC	3	3	4	3	2	3	2	3	2	2	2	2
CCHP	1	4	2	4	4	4	4	4	1	1	1	1

Energy Cost	B1		B2		L1		L2		K1		K2	
	C	V	C	V	C	V	C	V	C	V	C	V
All-electric Grid	4	4	2	4	2	3	2	3	1	1	1	1
Electric + NG Grid	3	2	3	2	4	1	4	1	2	2	4	2
DHC	2	3	4	3	3	2	3	2	3	3	3	3
CCHP	1	1	1	1	1	4	1	4	4	4	2	4

C = Constant-efficiency Model, V = Variable-efficiency Model

3.2 Neighborhood Results Using Variable Models

This section highlights the key results from applying the variable-efficiency models to the six neighborhood designs. Figure 8 summarizes the annual energy consumption for each of the neighborhoods by energy supply strategy. Overall, the Lisbon neighborhoods situated in mild climates consume the smallest amount of energy, while the Kuwait neighborhoods consume the most. Heating loads represent a significant fraction of the total energy use in Boston and Lisbon, whereas cooling needs dominate in Kuwait's warm climate.

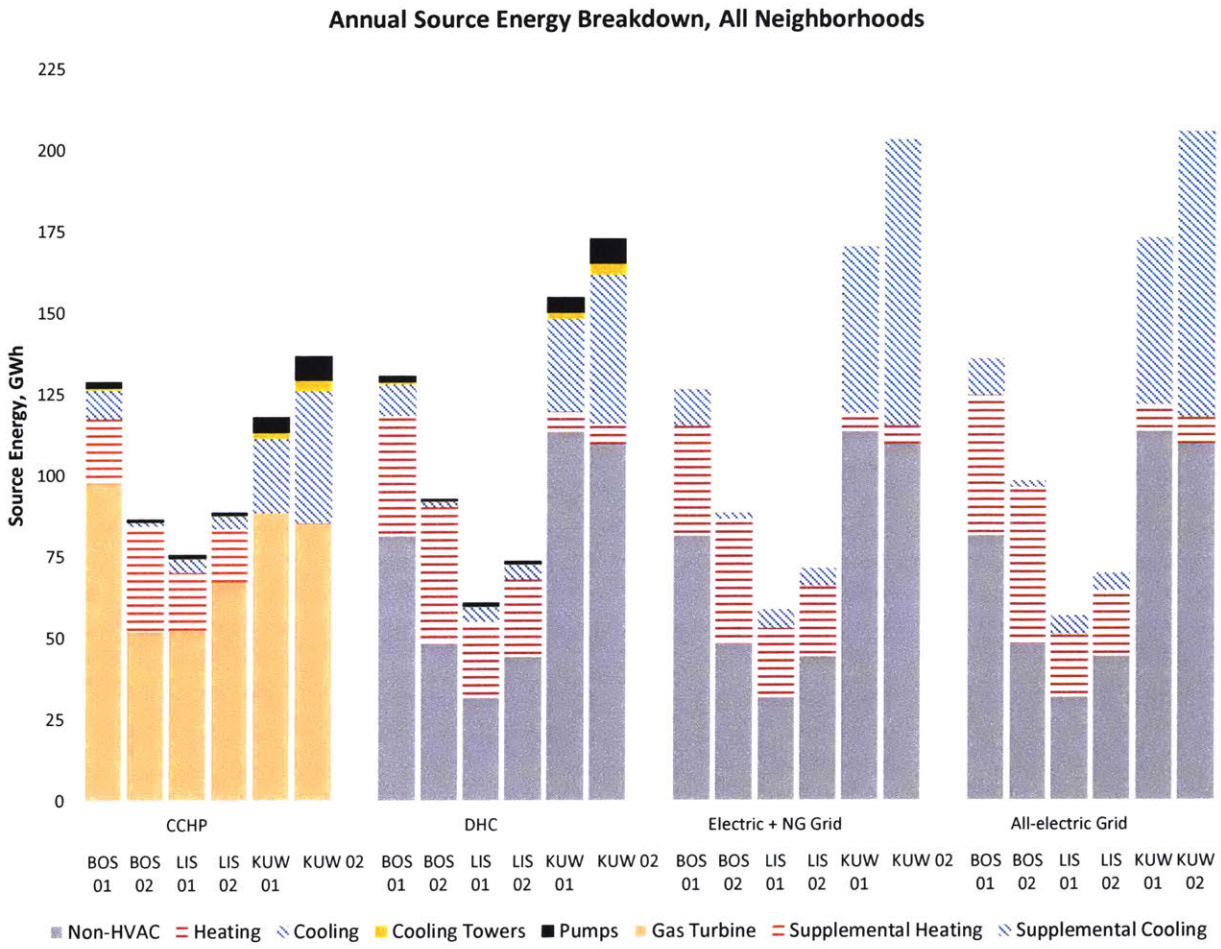

Figure 8: Energy Use Breakdown for Each Neighborhood by Strategy Showing Differences in Total Source Energy

Except for the two Boston neighborhoods' total input energy, the best energy supply strategies with respect to energy, emissions, and cost were identical for the two neighborhoods in the same city. Given that the pairings share weather, emissions factors, energy costs, and electrical transmission losses, it is not surprising that the optimal energy supply schemes were nearly the same.

However, because of the dramatic regional differences, the optimal energy supply system varies between cities and with respect to the highlighted metrics. See Figure 8 for a summary of the annual results by neighborhood.

The ideal energy supply strategy for a given neighborhood differs depending on the relative importance of minimizing input energy, emissions, or energy costs. For example, look at the second neighborhood in Boston. The CCHP plant requires the smallest annual energy consumption, but if the primary goal is to minimize carbon emissions, the Electric + Natural Gas Grid energy supply strategy offers better performance.

While the best choice for minimal annual energy consumption and carbon emissions matches for five of the six case studies—all except the first Boston neighborhood—interestingly, the supply schemes with lowest energy costs are different for the same five examples. The two Kuwait City neighborhoods illustrate a dramatic inconsistency between energy use and cost. Despite requiring more than 50% more annual energy than the CCHP option, the All-electric grid scenario is 26x cheaper because of heavily subsidized electricity rates that do not reflect the true cost of electrical generation.

Small differences (approximately 5% or less) exist between the majority of the four energy supply strategies as shown in Table 7. For example, look at the first Boston neighborhood. The Electric + NG Grid scenario is predicted to require 6.9% less energy than the All-electric Grid option, but the predicted energy consumption for the DHC and CCHP options differs from this one by only 3.1% and 1.9%, respectively. A similar trend exists for the remaining three neighborhoods in Boston and Lisbon, where the difference between the most energy intensive scenario and the next is over 5%, but the remaining three options are within ~5% of each other. However, the Kuwait neighborhoods are a bit different. There, a small ~1.5% difference in predicted energy consumption exists for the All-electric and Electric + NG options, but larger differences on the order of 10-30% exist for the DHC and CCHP scenarios.

Three of the four energy supply scenarios are the best choice for at least one combination of neighborhood and key metric, but the third scenario with the district heating and cooling plant is absent in the results. Additional details are provided in the discussion section on this topic.

Table 7: Annual Energy, emissions, and energy cost results by neighborhood (optimal strategy bolded). % Column represents the percent difference between the current and largest value within a neighbourhood.

	Boston 01		Boston 02		Lisbon 01		Lisbon 02		Kuwait City 01		Kuwait City 02	
Input Energy (GWh)	Value	%	Value	%	Value	%	Value	%	Value	%	Value	%
All-electric Grid	135.4	0.0%	97.8	0.0%	**56.5**	-25.0%	**69.5**	-21.4%	172.7	0.0%	205.5	0.0%
Electric + NG Grid	**126.1**	-6.9%	88.2	-9.9%	58.4	-22.5%	71.0	-19.7%	170.0	-1.5%	203.0	-1.2%
DHC	130.3	-3.8%	92.6	-5.3%	60.4	-19.7%	73.4	-17.0%	154.4	-10.6%	172.4	-16.1%
CCHP	128.6	-5.0%	**86.3**	-11.8%	75.3	0.0%	88.5	0.0%	**117.7**	-31.8%	**136.6**	-33.5%

	Boston 01		Boston 02		Lisbon 01		Lisbon 02		Kuwait City 01		Kuwait City 02	
Emissions (x100 MT CO^2)	Value	%	Value	%	Value	%	Value	%	Value	%	Value	%
All-electric Grid	201.1	-10.8%	145.2	-5.9%	**76.6**	-42.1%	**94.3**	-39.7%	337.8	0.0%	402.0	0.0%
Electric + NG Grid	**198.3**	-12.0%	**143.4**	-7.1%	88.8	-32.9%	106.1	-32.1%	331.8	-1.8%	396.3	-1.4%
DHC	204.5	-9.2%	151.0	-2.1%	92.2	-30.3%	110.0	-29.7%	297.4	-12.0%	330.0	-17.9%
CCHP	225.4	0.0%	154.3	0.0%	132.3	0.0%	156.3	0.0%	**204.4**	-39.5%	**233.5**	-41.9%

	Boston 01		Boston 02		Lisbon 01		Lisbon 02		Kuwait City 01		Kuwait City 02	
Energy Cost (Million USD)	Value	%	Value	%	Value	%	Value	%	Value	%	Value	%
All-electric Grid	$7.69	0.0%	$5.55	0.0%	$6.80	-9.3%	$8.38	-4.9%	**$0.16**	-96.8%	**$0.19**	-96.1%
Electric + NG Grid	$6.53	-15.0%	$4.29	-22.7%	**$6.59**	-12.1%	**$8.11**	-8.0%	$0.48	-90.8%	$0.53	-89.4%
DHC	$6.68	-13.2%	$4.47	-19.5%	$6.77	-9.7%	$8.33	-5.5%	$0.49	-90.5%	$0.53	-89.4%
CCHP	**$4.98**	-35.2%	**$3.29**	-40.8%	$7.50	0.0%	$8.81	0.0%	$5.15	0.0%	$4.98	0.0%

The overall heating and cooling system efficiencies for each energy supply scheme and neighborhood can be found in Table 8. The Electric Grid + NG strategy performed the best for overall heating efficiency for Boston and Kuwait City. This is likely because no heat losses were assumed for this scenario in comparison to the two district-level systems. While the heat pumps in the all-electric scheme have a higher COP than the boilers, the total system efficiency accounts for the electrical generation efficiency and transmission losses which reduce the overall performance of the heating system.

Lisbon's electrical grid is significantly more efficient than Boston's and Kuwait City's, and, as a result, the All-Electric Grid wins for heating performance for the two neighborhoods in Portugal. Except for the second neighborhood in Boston, the CCHP plant performs with the highest cooling efficiency. This is the result of coupling high-efficiency centrifugal chillers with absorption chillers that take advantage of waste heat. The waste heat is not subject to the electrical generation efficiency or transmission losses that decrease the overall system efficiency of cooling systems in the other three scenarios.

Table 8: Heating and Cooling System Efficiencies by Energy Supply Strategy and Neighborhood

Heating System Efficiency	**B1**	**B2**	**L1**	**L2**	**K1**	**K2**
All-electric Grid	0.54	0.55	0.75	0.73	0.47	0.48
Electric + NG Grid	0.68	0.69	0.69	0.68	0.69	0.69
DHC	0.63	0.63	0.63	0.63	0.63	0.63
CCHP	0.55	0.55	0.59	0.58	0.48	0.48
Cooling System Efficiency	**B1**	**B2**	**L1**	**L2**	**K1**	**K2**
All-electric Grid	1.89	1.97	2.43	2.52	0.98	0.93
Electric + NG Grid	1.89	1.97	2.43	2.52	0.98	0.93
DHC	1.85	1.73	2.57	2.54	1.50	1.52
CCHP	2.21	1.87	3.02	2.84	1.74	1.80

4 DISCUSSION

The application of the energy supply systems framework to the six case studies highlighted the implications of using variable-efficiency energy supply models over constant COP models, as well as the variability in the optimal energy supply system depending on objective and the regional power generation characteristics.

4.1 Constant vs. Variable Results

Figure 6 illustrates the double-digit percentage variance between the two types of models for the Boston and Lisbon neighborhoods, and a mid to high single-digit variance for the case studies located in Kuwait City. While these results alone should convince the reader that the type of model used matters, Figure 7 reinforces this observation. For the six case studies the authors used, the CCHP plant and All-electric Grid scenarios exhibited the greatest variance between the constant and variable models. It is not surprising that the CCHP scenarios illustrated the greatest variance, as they rely on the most equipment models. Naturally, the potential for differences to accumulate increases with a larger number of equipment models. However, it is not as obvious why the All-electric Grid scenario exhibits more than double the difference that the DHC and Electric + Natural Gas Grid scenarios display.

The summary of the results by equipment type in Table 5 help explain the dramatic difference for the All-electric scenario which relies on electric, air-source heat pumps for both heating and cooling. Of the six variable-efficiency equipment models implemented, these two models exhibited the greatest difference in COP in comparison to their constant-efficiency counterparts.

Though the differences in the results for the Electric Grid + NG scenario are all under 4%, the authors caution readers who may be tempted to conclude that the use of variable- or constant- efficiency models may not matter for this case. While this conclusion may be valid for the six case studies examined in this text, this trend may not generalize well to other neighborhoods. The close agreement between the two model types for this scenario is because the variable-efficiency heat pump in cooling mode's average COP is higher than its counterpart, whereas the natural gas boiler has the opposite trend. Together, these trends convey an artificial sense of agreement between the model types. However, if the ratio of heating to cooling loads were to dramatically change, the authors do not expect these trends to persist.

It is clear from Table 5 that equipment models exhibited double-digit differences in average variable COPs compared to their nominal, rated values. However, it is interesting to note that relatively small variance between neighborhoods for the COP of the gas boiler, absorption chiller, and gas turbine. The maximum difference between their average COP was 6.5%, 2.1%, and 1.5%. For these given models, it may not be necessary to estimate the equipment's COP on an hourly timescale. Instead, one may be able to use a constant-based COP model with little impact on the results. However, before arriving at this conclusion, the authors recommend confirming the models they selected for these pieces of equipment are appropriate for a wider set of cases and testing the models on a wider variety of neighborhoods to strengthen confidence in this trend.

The comparison between the constant- and variable-efficiency models undoubtedly shows a difference in the predicted energy consumption, carbon emissions, and energy cost. These differences were shown to have a material impact on the optimal energy supply strategy, but the obvious question is which type of models should be

used. Without a set of data from actual neighborhoods to compare, the authors cannot definitively guarantee one type of model is preferred. However, variable efficiency models capture the changes in efficiency from temperature and/or load that the constant-efficiency models neglect, bolstering their case for use. Additionally, the variable-efficiency models have been thoroughly documented and peer reviewed, which further strengthens their credibility and justification for use.

4.2 Neighborhood-level Results

The results presented demonstrate the influence that the regional characteristics of an area have on the optimal choice of an energy supply strategy. While it may seem obvious that energy supply systems should be evaluated within the context of their environment, these results provide empirical basis for this task.

As mentioned in the results section, the best energy supply strategy depends on the relative importance of minimizing total energy consumption, emissions, or energy costs. For the case studies evaluated in this text, the optimal strategy with respect to annual energy consumption and emissions were identical for five out of the six examples. This result is because all scenarios are tied to the combustion of carbon-releasing fuels. However, as renewable, low-carbon energy sources are increasingly integrated into electric grids, the authors expect this trend to change.

4.2.1 Boston Neighborhoods

The authors' models predict that the All-electric and CCHP options are the optimal strategy for the first and second Boston neighborhoods with respect to total input or source energy. However, as noted in the previous section, the difference between these two options and the DHC option is less than 5%. Depending on how closely the parameters and equipment used match an actual neighborhood in Boston, 5% may not be a large enough difference to declare a clear winner based on energy alone. But, comparing the carbon and cost metrics provides additional information that can be used to make a decision. For example, due to the disparity in electricity and natural gas costs in Boston, the CCHP plant is dramatically cheaper than the other three options that rely more on electricity from the grid.

Assuming that a 5% or greater difference is needed to reasonably say one scenario is different than another, the authors conclude that the All-electric option should not be selected, but the other three options are possible choices. However, as the electrical grid in Boston becomes more energy efficient, this option will become more attractive. From an emissions standpoint, the first three options perform similarly (All-electric, Electric + NG grid, and DHC). However, the CCHP performs the worst by a fare margin.

4.2.2 Lisbon Neighborhoods

Three different options are viable top candidates with respect to both input energy and cost if one assumes that +/- 5% is too close to definitively decide. For emissions, the choice is clearer and the all-electric grid wins. The primary driver for this result is the high percentage of renewable, low-carbon energy sources. Given this, the authors note that the All-electric scenario is likely the best all-around strategy for Lisbon.

4.2.3 Kuwait City Neighborhoods

If minimizing energy consumption and emissions are the key objectives, the authors recommend the use of a CCHP, which is predicted to significantly outperform the other three scenarios. This is because of the combination of low-efficiency, fossil-burning power plants used in Kuwait. However, the dramatically subsidized electricity rates favor the use of an All-electric system.

All scenarios took first place for at least one combination of neighborhood and key metric, except for the district heating and cooling plant—though it should be noted that the DHC plant took second place for the Kuwait City neighborhoods with respect to input energy and carbon emissions. The authors expect DHC plants to continue to play an integral role in the global energy supply system, despite these results for several reasons. With the increasing integration of low-carbon electrical sources, the DHC plant will become more attractive from an emissions standpoint relative to its CCHP counterpart. Additionally, the replacement of the district-scale gas boilers with heat pumps will further improve the energy and emissions performance of the DHC plant.

5 CONCLUSIONS AND FUTURE WORK

The primary contributions of this work are: (1) Development of an integrated energy supply and demand analysis tool, (2) Comparison between constant- and variable-efficiency supply models, and (3) Results from six neighborhood case studies.

The application of the authors' integrated energy supply tool to the six neighborhood designs reveals several key takeaways. First, constant- and variable-efficiency energy supply models often produce directionally different results with respect to energy, carbon, and cost. Second, the optimal energy supply scheme is non-trivial and depends on the relative importance of energy, carbon, and cost, in addition to region-specific parameters. Additionally, while the optimal strategy may not be clear based on the results, often at least one of the energy supply strategies can be eliminated from consideration.

The authors identified several areas of focus that may improve the framework presented in this manuscript. The first is conducting a comparison of the predictions made by the energy supply strategies to an actual neighborhood's energy consumption. This analysis will benchmark the variance between the predicted and actual energy consumption and determine the need for calibration of the energy supply models.

A second is expanding the modularity of the equipment models, allowing users to construct more complex, customizable energy supply systems. For future work, the authors recommend including a modified district heating and cooling scenario that uses large heat pumps (>1 MW), the ability to utilize economizing by using thermal reservoirs, and the inclusion of thermal storage and heat exchange between buildings.

The authors also suggest additional work to determine if the constant heat losses assumption for the DHC and CCHP strategies is appropriate. Finally, the authors see strong benefits associated to including functionality for estimating investments costs that would enable more sophisticated financial comparisons of energy supply schemes.

The proposed framework represents an improvement in coupling supply and demand analyses, and the authors hope this tool will help municipalities, developers, and urban planners focus their attention on the most promising energy supply strategies.

6 APPENDIX

6.1 Equipment Parameters

Table 9: Heat Pump (Cooling Mode) Specifications

Make	Mitsubishi
Model	MUZ-A09NA-1 (outdoor unit) and MSZ-A09NA (indoor unit)
Rated Cooling Capacity	9 kW (2.6 Refrigeration Tons)
Nominal COP	3.81
PLR range	10% to 100%
Zone - Outdoor air differential range	0C to 30C
Evaporator Outlet Air Temeprature	12.5 °C, Saturdated

Table 10: Heat Pump (Heating Mode) Coefficients

Coefficients	Values
C0	0.0914
C1	0.8033
C2	2.5976
C3	-3.2925
C4	-0.8678
C5	0.1902
C6	1.4833

Table 11: Heat Pump (Heating Mode) Specifications

Make	Fujitsu
Model	ASU12RLS (indoor unit) AOU12RLS (outdoor unit)
Rated Heating Capacity	4.69 kW (1.3 RT)
Nominal COP	3.90
Outdoor air drybulb temperature range	-14 to 18 °C
PLR range	28% to 100%
Indoor Zone Temperature	Constant 21 °C

Table 12: Hydronic Boiler Coefficients

Coefficients	Values
c1	0.83888652
c2	0.132579019
c3	-0.17028503
c4	0.047468326

Table 13: McQuay PEH Electric Centrifugal Chiller Coefficients

Coefficients	CapFunT	EIRFunT	EIRFPLR
a	5.52E-01	4.45E-01	1.04E-01
b	1..39E-02	-3.19E-02	1.71E-02
c	-4.82E-03	-8.26E-04	-1.40E-05
d	3.710E-02	3.71E-02	-9.14E-03
e	-1.43E-03	-4.89E-05	1.08
f	3.47E-03	-4.98E-04	-1.63E-02
g	-	-	0
h	-	-	-1.81E-01
i	-	-	0
j	-	-	0

Table 14: Electric Centrifugal Chiller Specifications

Make	McQuay
Model	PEH
Rated Capacity	819 kW
Nominal COP	8.11
Min Part Load Ratio	9%
Min Leaving Evap Temp	4.44 °C
Max Leaving Evap Temp	8.89 °C
Min Leaving Condenser Temp	18.51 °C
Max Leaving Condenser Temp	35.07 °C

Table 15: Leaving Condenser Water Return Temperature Approximation Coefficients

Coefficients	Values
C1	28.27
C2	5.57 E-04
C3	1.63 E-01

Table 16: Absorption Chiller Coefficients

Coefficients	AbsCapFunT	TFIRFunT	TeEIRFunPLR
a	-1.15	1.31E+00	2.63E-02
b	-8.01E-02	-1.59E-02	6.78E-01
c	-9.45E-03	7.74E-04	2.74E-01
d	2.10E-01	-1.96E-02	-
e	-5.67E-03	3.78E-04	-
f	9.44E-03	5.58E-05	-

Table 17: Absorption Chiller Specifications

Make	Unknown
Model	Unknown
Rated Cooling Capacity	231 kW (66.0 Refrigeration Tons)
Nominal COP	1.39
Outdoor air drybulb temperature range	-14 to 18 °C
PLR range	0% to 100%

6.2 Regional Information

Table 18: Electrical Generation Efficiencies from U.S. Energy Information Administration

Prime Mover	Fuel Type	Efficiency
Gas Turbine	Natural Gas	30%
Gas Turbine	Petroleum	25%
Combined Cycle	Natural Gas	45%
Combined Cycle	Petroleum	35%
Steam Turbine	Nuclear	33%
Steam Turbine	Coal	34%
Geothermal	-	16%
Hydro	-	90%
Solar Photovoltaic	-	12%
Solar Thermal	-	21%
Wind	-	26%

Table 19: Power Generation Mix by City

Electricity Sources	Boston	Lisbon	Kuwait City
Coal	25%	23%	0%
Nuclear	13%	0%	0%
Natural Gas	53%	13%	34%
Petroleum	2%	3%	66%
Biomass	3%	5%	0%
Hydro	3%	31%	0%
Photovoltaic	0%	1%	0%
Geothermal	0%	<1%	0%
Other	1%	0%	0%

Sources: Boston (IER, 2009), Lisbon (IEA, 2014), and Kuwait City (IEA, 2014)

Table 20: Region-specific Parameter Sources

Input Parameters	Boston	Lisbon	Kuwait City
Price of Electricity (USD/kWh)	EIA, 2017	Eurostat, 2016	Oxford, 2014
Price of Natural Gas (USD/kWh)	BLS, 2017	Eurostat, 2016	Mundi, 2017
Electrical Transmission Losses (%)	EIA, 2017	IEA, 2013	IEA, 2014
Emissions Factor (Metric Tons CO2/kWh generated)	Emissions Factors	Emissions Factors	Emissions Factors

7 References

2012_energy_roadmap_2050_en_0.pdf. (n.d.). Retrieved from https://ec.europa.eu/energy/sites/ener/files/documents/2012_energy_roadmap_2050_en_0.pdf

Average Energy Prices In Boston-Brockton-Nashua – February 2017 : New England Information Office : U.S. Bureau of Labor Statistics. (n.d.). Retrieved April 17, 2017, from https://www.bls.gov/regions/new-england/news-release/averageenergyprices_boston.htm

Bertagnolio, S. (2012). Evidence-based model calibration for efficient building energy services. Université de Liège, Liège, Belgium. Retrieved from http://orbi.ulg.ac.be/handle/2268/125650

Cheung, H., & Braun, J. (2010). Performance Characteristics and Mapping for a Variable-Speed Ductless Heat Pump. International Refrigeration and Air Conditioning Conference. Retrieved from http://docs.lib.purdue.edu/iracc/1124

Chicco, G., & Mancarella, P. (2008). Assessment of the greenhouse gas emissions from cogeneration and trigeneration systems. Part I: Models and indicators. Energy, 33(3), 410–417. https://doi.org/10.1016/j.energy.2007.10.006

CitySim Software. (n.d.). Retrieved from http://citysim.epfl.ch

Committee on Climate Change. (2016). Next steps for UK heat policy. Retrieved from https://www.theccc.org.uk/wp-content/uploads/2016/10/Next-steps-for-UK-heat-policy-Committee-on-Climate-Change-October-2016.pdf

Connolly, D., Lund, H., Mathiesen, B. V., Werner, S., Möller, B., Persson, U., … Nielsen, S. (2014). Heat Roadmap Europe: Combining district heating with heat savings to decarbonise the EU energy system. Energy Policy, 65, 475–489. https://doi.org/10.1016/j.enpol.2013.10.035

Creutzig, F., Baiocchi, G., Bierkandt, R., Pichler, P.-P., & Seto, K. C. (2015). Global typology of urban energy use and potentials for an urbanization mitigation wedge. Proceedings of the National Academy of Sciences, 112(20), 6283–6288. https://doi.org/10.1073/pnas.1315545112

District Energy in Cities :: Our Planet. (n.d.). Retrieved April 16, 2017, from http://web.unep.org/ourplanet/october-2016/unep-publications/district-energy-cities

District Energy in Cities: Unlocking the Potential of Energy Efficiency and Renewable Energy. (n.d.). United Nations Environment Programme (UNEP). Retrieved from http://www.unep.org/energy/portals/50177/DES_District_Energy_Report_full_02_d.pdf

Dogan, T., & Reinhart, C. (2017). Shoeboxer: An algorithm for abstracted rapid multi-zone urban building energy model generation and simulation. Energy and Buildings, 140, 140–153. https://doi.org/10.1016/j.enbuild.2017.01.030

EIA. (2017a, February). FAQ: How much electricity is lost in transmission and distribution in the United States? Retrieved from https://www.eia.gov/tools/faqs/faq.php?id=105&t=3

EIA. (2017b, March). Table 5.6.A. Average Price of Electricity to Ultimate Customers by End-Use Sector,. Retrieved from https://www.eia.gov/electricity/monthly/epm_table_grapher.cfm?t=epmt_5_6_a

Emissions Factors. (2017). Emissions Factors. Retrieved from https://emissionfactors.com/factors/

Energy – UN-Habitat. (n.d.). Retrieved April 15, 2017, from https://unhabitat.org/urban-themes/energy/

Energy Information Administration. (2011). Appendix F: Alternatives for Estimating Energy Consumption. Retrieved from https://www.eia.gov/totalenergy/data/annual/pdf/sec17.pdf

Energy Information Administration. (2015). Table 8.2. Average Tested Heat Rates by Prime Mover and Energy Source, 2007 - 2015. Retrieved from https://www.eia.gov/electricity/annual/html/epa_08_02.html

EngineeringReference.pdf. (n.d.). Retrieved from https://energyplus.net/sites/default/files/pdfs_v8.3.0/EngineeringReference.pdf

Eurostat. (2016, July). Energy Price Statistics. Retrieved from http://ec.europa.eu/eurostat/statistics-explained/index.php/Energy_price_statistics

Fattouh, B., Mahadeva, L., & Oxford Institute for Energy Studies. (2014). Price reform in Kuwait's electricity and water sector: assessing the net benefits in the presence of congestion.

Fonseca, J. A., Nguyen, T.-A., Schlueter, A., & Marechal, F. (2016). City Energy Analyst (CEA): Integrated framework for analysis and optimization of building energy systems in neighborhoods and city districts. Energy and Buildings, 113, 202–226. https://doi.org/10.1016/j.enbuild.2015.11.055

Frederiksin, S., & Werner, S. (2013). District Heating and Cooling.

Gang, W., Wang, S., Xiao, F., & Gao, D. (2016). District cooling systems: Technology integration, system optimization, challenges and opportunities for applications. Renewable and Sustainable Energy Reviews, 53, 253–264. https://doi.org/10.1016/j.rser.2015.08.051

GE Power. (2016). LM6000 Power Plants (50/60 Hz). Retrieved from https://powergen.gepower.com/content/dam/gepower-pgdp/global/en_US/documents/product/gas%20turbines/Fact%20Sheet/2017-prod-specs/lm6000-power-plants.pdf

Handbook | ashrae.org. (n.d.). Retrieved April 16, 2017, from https://www.ashrae.org/resources--publications/handbook

Hydeman, M., Webb, N., Sreedharan, P., & Blanc, S. (2002). Development and testing of a reformulated regression-based electric chiller model. ResearchGate, 108, 1118–1127.

Institute for Energy Research. (2009). Massachusetts Energy Facts. Retrieved from http://instituteforenergyresearch.org/media/state-regs/pdf/Massachusetts.pdf

International Energy Agency. (2013). Portugal: Electricity and Heat for 2013. Retrieved from http://www.iea.org/statistics/statisticssearch/report/?country=PORTUGAL&product=electricityandheat&year=2013

International Energy Agency. (2014a). Kuwait: Electricity and Heat for 2014. Retrieved from http://www.iea.org/statistics/statisticssearch/report/?country=KUWAIT&product=electricityandheat&year=2013

International Energy Agency. (2014b). Linking Heat and Electricity Systems (p. 62). Retrieved from https://www.iea.org/publications/freepublications/publication/LinkingHeatandElectricitySystems.pdf

International Energy Agency. (2014c). Portugal: Electricity and Heat for 2014. Retrieved from https://www.iea.org/statistics/statisticssearch/report/?country=PORTUGAL&product=electricityandheat&year=2014

Keirstead, J., Jennings, M., & Sivakumar, A. (2012). A review of urban energy system models: Approaches, challenges and opportunities. Renewable and Sustainable Energy Reviews, 16(6), 3847–3866. https://doi.org/10.1016/j.rser.2012.02.047

Lebrun, J., Silva, C. A., Trebilcock, F., & Winandy, E. (2004). Simplified models for direct and indirect

contact cooling towers and evaporative condensers. Building Services Engineering Research and Technology, 25(1), 25–31. https://doi.org/10.1191/0143624404bt088oa

Mancarella, P. (2012). Distributed multi-generation options to increase environmental efficiency in smart cities. In 2012 IEEE Power and Energy Society General Meeting (pp. 1–8). https://doi.org/10.1109/PESGM.2012.6345129

Meybodi, M. A., & Behnia, M. (2011). Optimum Sizing of the Prime Mover in a Medium Scale Gas Turbine CHP System. Journal of Engineering for Gas Turbines and Power, 133(11), 112001. https://doi.org/10.1115/1.4003670

Natural Gas - Monthly Price - Commodity Prices - Price Charts, Data, and News - IndexMundi. (n.d.). Retrieved April 17, 2017, from http://www.indexmundi.com/commodities/?commodity=natural-gas

Pilavachi, P. A. (2000). Power generation with gas turbine systems and combined heat and power. Applied Thermal Engineering, 20(15), 1421–1429. https://doi.org/10.1016/S1359-4311(00)00016-8

Reinhart, C., Dogan, T., Jakubiec, J. A., Rakha, T., & Sang, A. (2013). Umi-an urban simulation environment for building energy use, daylighting and walkability. In 13th Conference of International Building Performance Simulation Association, Chambery, France. Retrieved from http://web.mit.edu/SustainableDesignLab/publications/umi_introduction.pdf

Reinhart, C. F., & Cerezo Davila, C. (2016). Urban building energy modeling – A review of a nascent field. Building and Environment, 97, 196–202. https://doi.org/10.1016/j.buildenv.2015.12.001

Rezaie, B., & Rosen, M. A. (2012). District heating and cooling: Review of technology and potential enhancements. Applied Energy, 93, 2–10. https://doi.org/10.1016/j.apenergy.2011.04.020

Robinson, D., Haldi, F., Kämpf, J., Leroux, P., Perez, D., Rasheed, A., & Wilke, U. (2009). CitySim: Comprehensive micro-simulation of resource flows for sustainable urban planning. In Proc. Building Simulation (pp. 1614–1627). Retrieved from https://infoscience.epfl.ch/record/148717/files/dr.bsCitySim%20BS09_1083_1090.pdf

Siemens - SGen-2000H Series Generators. (n.d.). [ctc_product]. Retrieved May 10, 2017, from https://www.energy.siemens.com/hq/en/fossil-power-generation/generators/sgen-2000h-series.htm#content=Technical%20data

Thornton, R. (2005). IDEA Report: The District Energy Industry. Retrieved from http://www.districtenergy.org/pdfs/IDEA_Industry_White_Paper.pdf

United Nations. (2015). World Urbanization Prospects. Retrieved from https://esa.un.org/unpd/wup/

United Nations. (n.d.). Sustainable Energy for All. Retrieved from http://www.se4all.org

U.S. Department of Energy. (n.d.). EnergyPlus Energy Simulation Software. Retrieved from http://apps1.eere.energy.gov/buildings/energyplus/

Werner, S. (n.d.). International review of district heating and cooling. Energy. https://doi.org/10.1016/j.energy.2017.04.045

Zakula, T. (2013). Model predictive control for energy efficient cooling and dehumidification (Thesis). Massachusetts Institute of Technology. Retrieved from http://dspace.mit.edu/handle/1721.1/8216